13th World Conference on Earthquake Engineering
Vancouver, B.C., Canada
August 1-6, 2004
Paper No. 731

NEW ATTENUATION FORMULA OF EARTHQUAKE GROUND MOTIONS PASSING THROUGH THE VOLCANIC FRONT

Nobuo TAKAI[1], Gaku SHIMIZU[2] and Shigeyuki OKADA[3]

SUMMARY

The attenuation relation of earthquake strong ground motion, which is predictable in wide area, is important. In this study, it was tried that the attenuation formula based on positional relation of volcanic front (VF), hypocenter and observation site was made. By requiring the regression formula for intra-plate earthquake by the division of hypocentral distance in the volcanic front, the attenuation formula, which the effect of the large-scale attenuation structure reflected, was obtained.

INTRODUCTION

Many experimental attenuation formulas for estimating of ground motions severity have been developed by means of regression analysis [1,2]. These formulas, however, are not adequate in estimating ground motions precisely, since the complex Q-value structure within subduction zones is not taken into consideration in these equations. On the other hand, it has been indicated that the distribution of earthquake motions greatly differs in the region divided in the volcanic front (V.F.: show Figure 1) in the effect of the Q-value structure. Especially, large earthquake occurred around Pacific plate boundary in Hokkaido frequently, and it became a cause of the damage in the wide area. Figure 2 shows the relation between epicentral distance and peak horizontal ground motion (PGA) of earthquake that occurred in Hokkaido. In two regions classified by the volcanic front, the tendency of the attenuation by the distance is greatly different, as it is clear from this figure. The objective of this study is to develop an attenuation formula based on the positional relation of V.F., hypocenters and the observation points.

METHODOLOGY

The volcanic front located in northern Japan is shown in Figure 1. The distance from the epicenter to V.F. ($\Delta 1$) and the distance from V.F. to the observation points ($\Delta 2$) is derived by dividing the hypocentral distances by V.F.. Next, the hypocentral distance is divided at the ratio of $\Delta 2$ and $\Delta 1$, and $R1$ ($=R*\Delta 1/\Delta$) and $R2$ ($=R*\Delta 2/\Delta$) for the regression analysis are required. Figure 3 shows the relation between epicenter,

[1] Research Associate, Graduate School of Engineering, Hokkaido University
[2] Graduate student, Graduate School of Engineering, Hokkaido University
[3] Associate Professor, Graduate School of Engineering, Hokkaido University

hypocenter, observation site, *R1, R2, Δ1, Δ2* and volcanic front. PGA and JMA instrumental seismic intensity data of the K-NET is used for the analysis. A regression analysis is performed for each earthquake, using PGA and seismic intensity as the response variable and the distances as the explanatory variables. The values derived from the analysis and the magnitudes are used for performing further regression analysis.

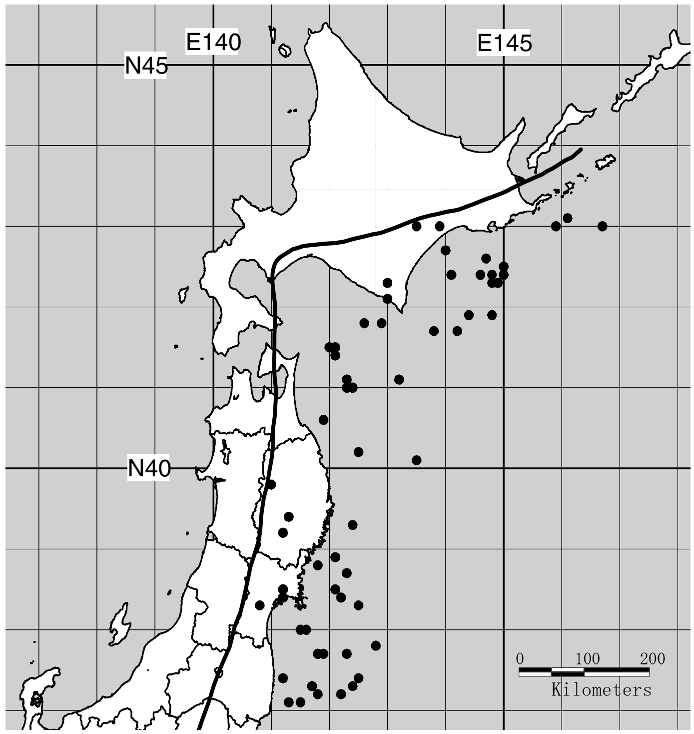

Figure 1. Target area and epicenter of earthquakes used in this study.
A solid line shows the volcanic front.

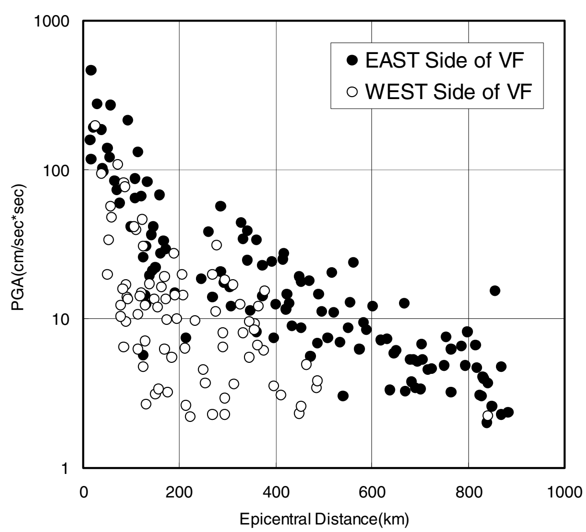

Fig.2 Relation between epicentral distance and peak horizontal ground acceleration (PGA) in NS component at Earthquake No.15 (shown in Table 1.) recorded by K-net.

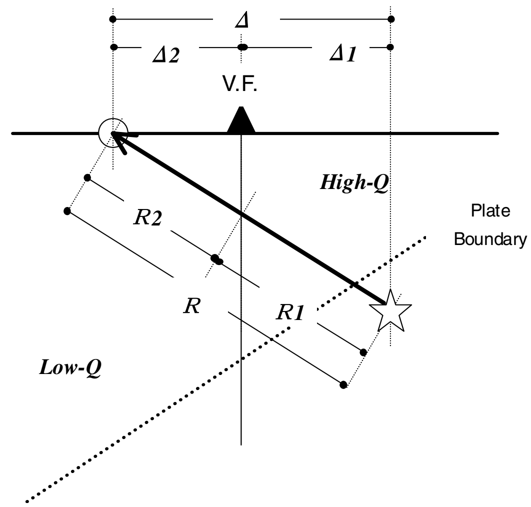

Figure 3. Projective transformation for real distance from epicentral distance.

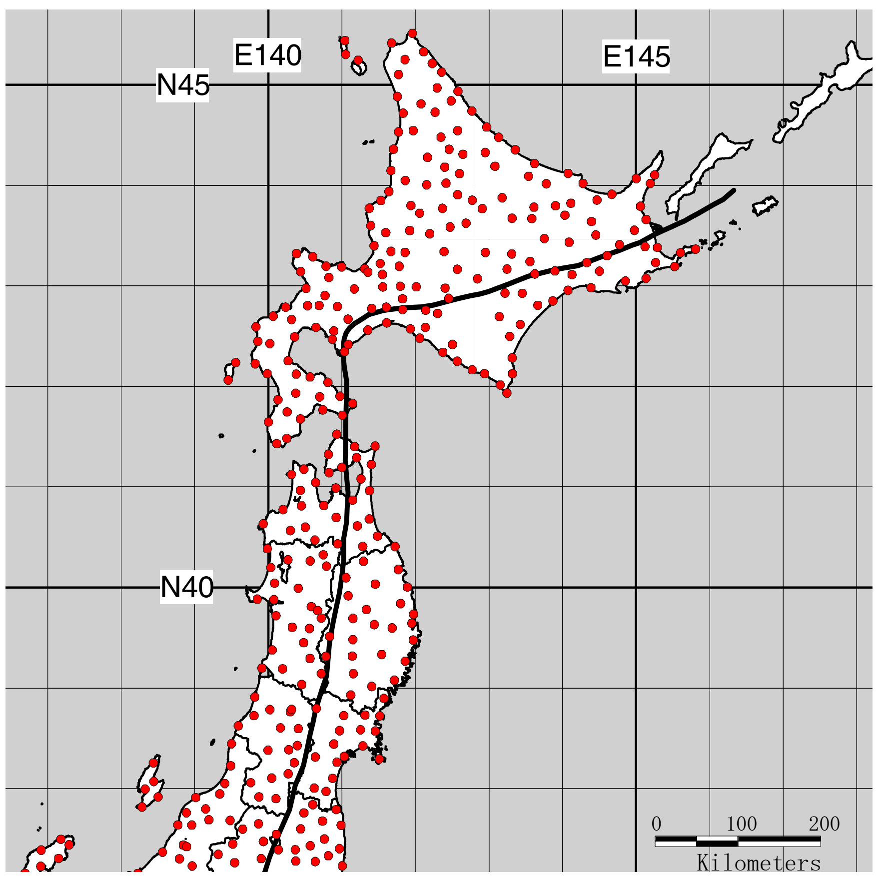

Figure 4. Distribution Map of K-NET observation sites.

Table 1. Table of earthquakes used in this study.
(Earthquakes for construction of prediction expression were shown with boldfaced type.)

No.	DATE	TIME (JST)	LAT (N)	LONGT (E)	Depth (km)	(MJ)	Region	Eq. Type
1	1997/2/20	16:55	41.8	142.9	49	5.9	S_OFF_URAKAWA	P
2	1997/5/12	7:59	37.1	141.3	54	5.7	E_OFF_FUKUSHIMA_PREF	P
3	1997/12/7	12:50	37.7	141.8	84	5.4	E_OFF_FUKUSHIMA_PREF	SP
4	1997/12/23	4:08	43	143.5	37	5.2	TOKACHI_REGION	P
5	1997/12/23	1:31	40.2	142.5	114	5.2	NE_OFF_IWATE_PREF	S
6	1998/1/31	0:50	41.4	142.1	62	5.3	E_OFF_AOMORI_PREF	P
7	1998/3/12	4:27	37.7	142.3	35	5.1	SE_OFF_MIYAGI_PREF	P
8	1998/5/21	6:54	38.5	142.1	84	5	E_OFF_MIYAGI_PREF	S
9	1998/8/16	23:05	37.2	141.8	42	5.3	E_OFF_FUKUSHIMA_PREF	P
10	1998/9/3	16:58	39.8	141	8	6.2	NORTHERN_IWATE_PREF	C
11	1998/9/15	16:24	38.3	140.8	13	5.2	SOUTHERN_MIYAGI_PREF	C
12	1998/11/24	4:48	38	141.6	83	5.2	SE_OFF_MIYAGI_PREF	P
13	1999/2/1	1:52	37.1	141.5	45	5.3	E_OFF_FUKUSHIMA_PREF	P
14	1999/3/19	2:55	41.1	143.2	29	5.8	E_OFF_AOMORI_PREF	P
15	**1999/5/13**	**2:59**	**43**	**143.9**	**106**	**6.3**	**KUSHIRO_REGION**	S
16	1999/10/5	9:39	37.4	142.5	57	5.2	SE_OFF_MIYAGI_PREF	P
17	1999/11/15	10:35	38.3	142.5	46	5.7	E_OFF_MIYAGI_PREF	P
18	2000/1/9	13:02	37.3	141.7	43	5.1	E_OFF_FUKUSHIMA_PREF	P
19	**2000/1/28**	**23:21**	**43**	**146.7**	**59**	**7**	**OFF_NEMURO_PENINSULA**	S
20	2000/3/20	6:26	38	141.5	78	5.1	SE_OFF_MIYAGI_PREF	SP
21	2000/7/1	5:34	37.3	141.7	42	5.2	E_OFF_FUKUSHIMA_PREF	P
22	2000/10/3	13:13	40.1	143.5	10	6	FAR_E_OFF_SANRIKU	P
23	2000/11/14	0:57	42.5	145	41	6.1	OFF_NEMURO_PENINSULA	P
24	2001/2/25	6:54	37.2	142.2	16	5.9	E_OFF_FUKUSHIMA_PREF	P
25	2001/4/3	4:54	40.6	141.9	63	5.6	E_OFF_AOMORI_PREF	SP
26	2001/4/12	16:02	37.3	141.7	44	5.1	E_OFF_FUKUSHIMA_PREF	P
27	**2001/4/27**	**2:49**	**43**	**145.9**	**80**	**5.9**	**OFF_NEMURO_PENINSULA**	S
28	2001/8/14	5:11	41	142.4	38	6.4	E_OFF_AOMORI_PREF	SP
29	2001/8/24	18:48	41	142.4	41	5.3	E_OFF_AOMORI_PREF	SP
30	2001/10/2	17:20	37.7	141.9	41	5.5	E_OFF_FUKUSHIMA_PREF	P
31	**2001/12/2**	**22:02**	**39.4**	**141.3**	**122**	**6.4**	**SOUTHERN_IWATE_PREF**	S
32	2002/1/27	16:09	39.3	142.4	46	5.5	E_OFF_IWATE_PREF	P
33	2002/2/14	10:12	41.5	142.1	64	5.1	E_OFF_AOMORI_PREF	SP
34	**2002/4/4**	**8:42**	**41.5**	**142**	**59**	**5.4**	**E_OFF_AOMORI_PREF**	S
35	2002/5/6	17:12	38.4	142.2	40	5	E_OFF_MIYAGI_PREF	P
36	2002/5/12	10:29	39.2	141.2	96	5.2	SOUTHERN_IWATE_PREF	S
37	2002/7/24	5:05	37.3	142.4	30	5.9	E_OFF_FUKUSHIMA_PREF	P
38	**2002/8/25**	**3:40**	**43.1**	**146.1**	**44**	**6**	**OFF_NEMURO_PENINSULA**	S
39	2002/10/14	23:13	41.1	142.3	53	6.1	E_OFF_AOMORI_PREF	SP
40	2002/11/3	12:37	38.9	142.1	46	6.3	KINKAZAN_REGION	P
41	2002/12/1	18:57	42.7	144	103	5.5	SE_OFF_TOKACHI	S
42	2002/12/5	0:50	38.7	142.3	40	5.3	E_OFF_MIYAGI_PREF	P
43	2003/2/16	12:03	37.4	141.2	63	5.2	E_OFF_FUKUSHIMA_PREF	SP
44	2003/3/3	7:47	37.7	141.8	41	5.9	E_OFF_FUKUSHIMA_PREF	P
45	2003/4/17	3:00	41	142.3	40	5.6	E_OFF_AOMORI_PREF	P
46	**2003/5/26**	**18:24**	**38.8**	**141.8**	**72**	**7.1**	**KINKAZAN_REGION**	S
47	2003/7/3	8:52	42.4	145	33	5.9	OFF_NEMURO_PENINSULA	S
48	2003/7/26	7:13	38.4	141.2	12	5.6	NORTHERN_MIYAGI_PREF	C
49	2003/7/26	0:13	38.4	141.2	12	6.4	NORTHERN_MIYAGI_PREF	C
50	2003/7/26	16:56	38.5	141.2	12	5.5	NORTHERN_MIYAGI_PREF	C
51	2003/7/28	4:08	38.5	141.2	14	5.1	NORTHERN_MIYAGI_PREF	C
52	2003/8/30	19:06	41.8	142.6	55	5.4	S_OFF_URAKAWA	P
53	2003/9/26	4:50	41.7	144.2	45	8	SE_OFF_TOKACHI	P
54	2003/9/26	6:08	41.7	143.8	21	7.1	SE_OFF_ERIMOMISAKI	P
55	2003/9/27	5:38	41.9	144.8	34	6	SE_OFF_TOKACHI	P
56	2003/9/28	7:23	42.1	143	51	5.2	HIDAKA_REGION	P
57	2003/9/29	11:37	42.4	144.6	43	6.5	SE_OFF_TOKACHI	P
58	2003/9/29	16:50	42.4	144.1	64	5.5	SE_OFF_TOKACHI	P
59	2003/10/8	18:07	42.6	144.7	51	6.4	SE_OFF_TOKACHI	P
60	2003/10/8	22:32	42.3	144.9	28	5.7	SE_OFF_TOKACHI	P
61	2003/10/11	9:08	41.9	144.4	28	6.1	SE_OFF_TOKACHI	P
62	2003/10/31	10:06	37.8	142.8	33	6.8	FAR_E_OFF_FUKUSHIMA_PREF	P
63	2003/11/24	21:18	42.3	143	52	5.3	HIDAKA_MOUNTAINS_REGION	P
64	2003/12/22	17:47	42.3	144.8	34	5.7	SE_OFF_TOKACHI	P
65	2003/12/29	10:31	42.4	144.8	39	6	SE_OFF_TOKACHI	P

Eq. Type
C: shallow **C**rustal earthquake
S: Intra-Plate(**S**lab) earthquake
P: Inter-**P**late earthquake
SP: The earthquake in which there was no classification **P** or **S**.

DATA

Kyoshin Net (K-NET) is the system that provides strong-motion data on the Internet web. The data are obtained at 1,000 observatories deployed all over Japan (Figure 4.). The average station-to-station distance is about 25km[3]. In this study, the analysis is carried out using the data of K-NET, and the target area is fixed in the Tohoku and the Hokkaido region (northern part of Japan). Under the condition that the magnitude is over 5.0 and the strong motion records are obtained at over 50 observatories, we select appropriate earthquakes as data used in this study from the earthquakes that occurred in and around the target area. Their seismic properties are shown in Table 1 and the epicenters are plotted in Figure 1. In Table 1 the key information in this study that is the type of earthquakes as shallow crustal, intra-plate, and inter-plate earthquakes is specified. The inter-plate earthquake and intra-plate earthquake were separated with focal depth, although there was no performance in classifying in some earthquakes clearly. The PGA used synthesis value of the 3 components, and measurement seismic intensity was calculated from the acceleration records of 3 components [4]. Since the effect of the ground amplification by surface geology at observatories is not neglected in this study, it takes into account that the final results may still remain affected by the ground amplification. The relationship between magnitude and hypocentral distance for all of the data is shown in Figure 5, which suggests that there is little correlation at magnitude and hypocentral distance, therefore the two stages regression analysis should be carried out.

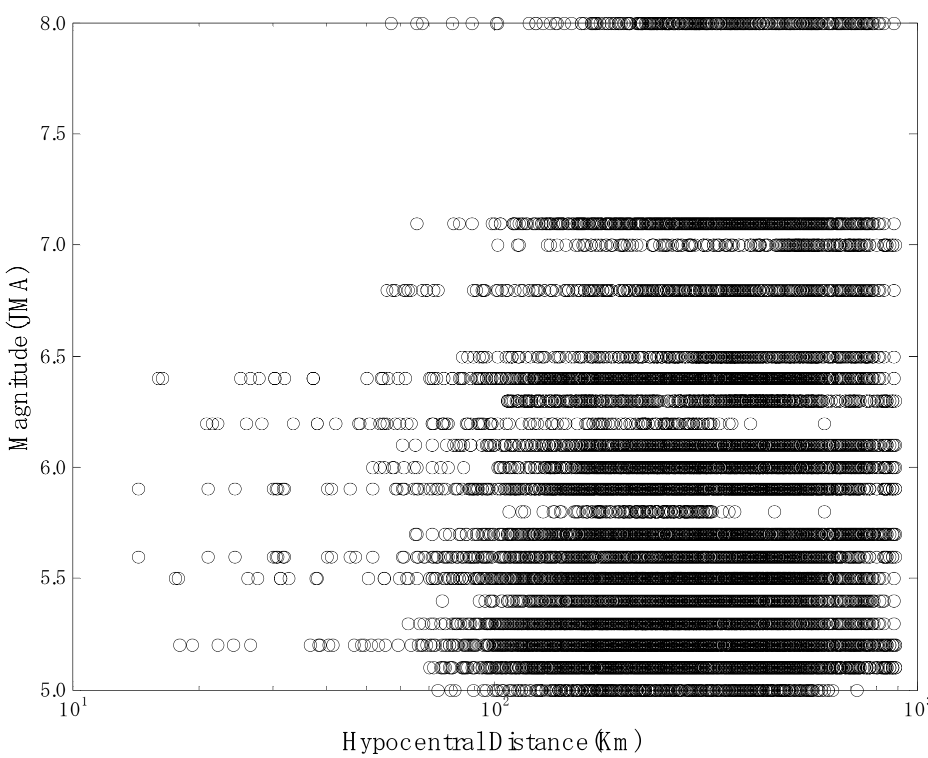

Fig.5 Relation between hypocentral distance and Magnitude for the earthquakes used in this study.

REGRESSION ANALYSIS

The examination of the all data

First, whether it improves the accuracy of the recurrence how much, when it returns in 2 variables, is examined. By returning in the equation under the sake that simplifies the problem, the comparison is carried out. PGA is regressed at formulas (1), (2), and seismic intensity at (3), (4).

$$\mathrm{Log}_{10}PGA=C_{1A1}-b_{1A1}R_1-b_{1A2}R_2 \qquad (1)$$

$$\mathrm{Log}10PGA=C_{1A0}-b_{1A0}R \qquad (2)$$

$$I=C_{1I1}-b_{1I1}R_1-b_{1I2}R_2 \qquad (3)$$

$$I=C_{1I0}-b_{1I0}R \qquad (4)$$

Where I is JMA intensity, C and b are regression coefficients. The form of equations are different on the prediction expression of under-mentioned and that they do not use the logarithms for the term of the regression, for examining the effect in 2 variables more in detail on these equations. Though it is clear that accuracy of determining improves both PGA and seismic intensity by choosing 2 variables (Figure 6), it can be understood that the dispersion is very large, when the ratio of the regression coefficients b_{1A1}, b_{1A2} are examined at earthquake focal depth and magnitude (Figure 7.).

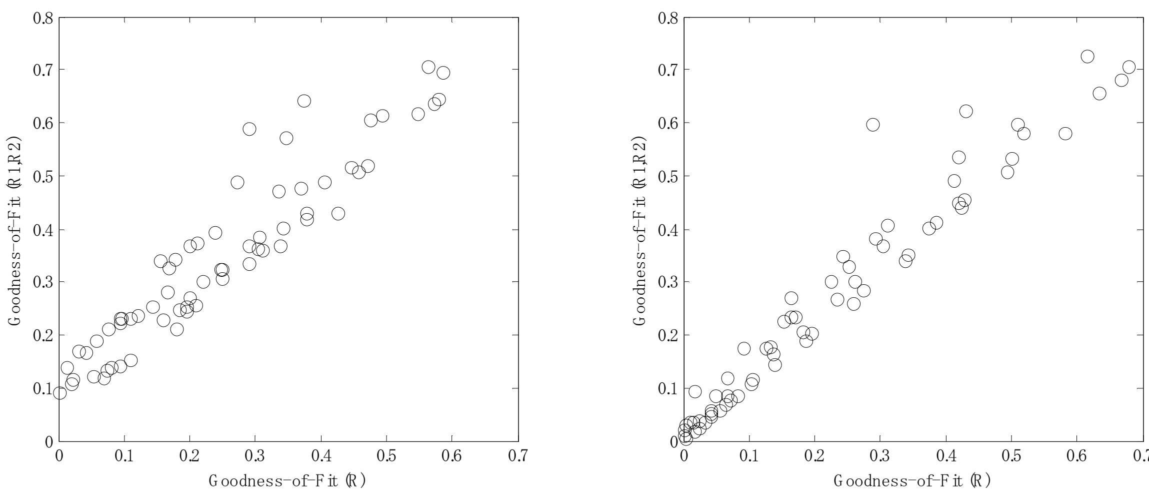

(a)PGA (b) JMA Instrumental Intensity

Figure 6. The comparison of each decision coefficient in the case of the regression analysis by 2 equations.

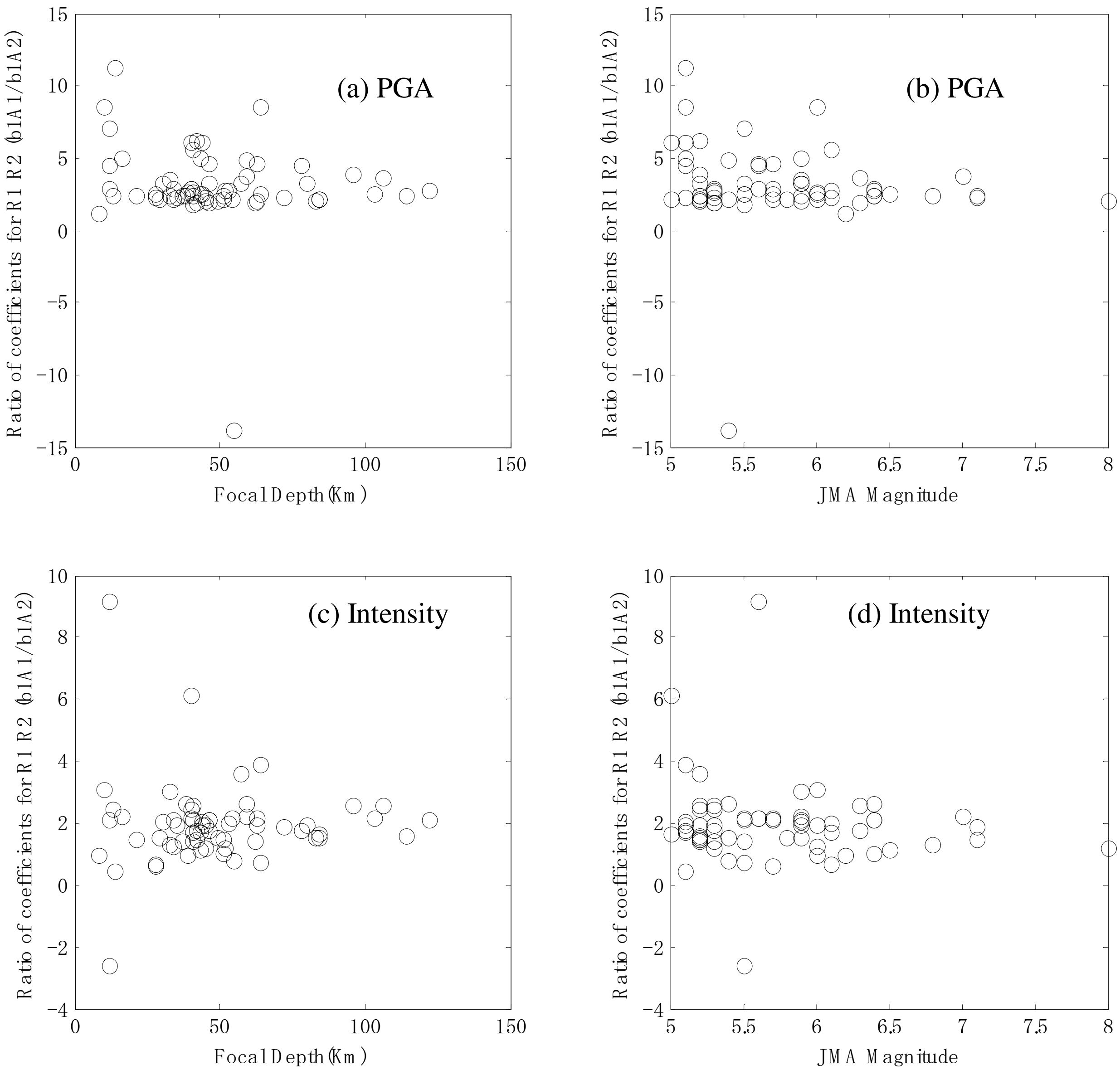

Figure 7. Relation between the ratio of coefficients b_{1A1}, b_{1A2} and (a)(c) focal depth, (b)(d) JMA Magnitude for all data.

Some causes of this dispersion are considered, and the polarization of the number of the observation point which held volcanic front seems to greatly contribute at the accuracy of the regression analysis. Therefore, in the selecting condition that is the proportion of both side sites number, the earthquakes for regression analysis are chosen again. As a result of trial and error, earthquakes in which the data in the Japan-sea side is over whole 40% are selected. In addition, the data whose hypocentral distance is within 500km are used. The regression analysis is carried out again under the condition above mentioned, and the ratio of the coefficient of *R1* and *R2* are compared with M, focal depth (Figure 8) and ratio of goodness-of-fit (Figure 9). Though ratios of the coefficient are not dependent on M (Figure 8(b)(d)), and it is seen, as the ratio of the deep coefficient as an earthquake are large (Figure 8(a)(c)). It can be clearly grasped that the accuracy of intra-plate earthquake drastically improves by making in 2 variables regression analysis, when the earthquake type classifies (Figure 9).

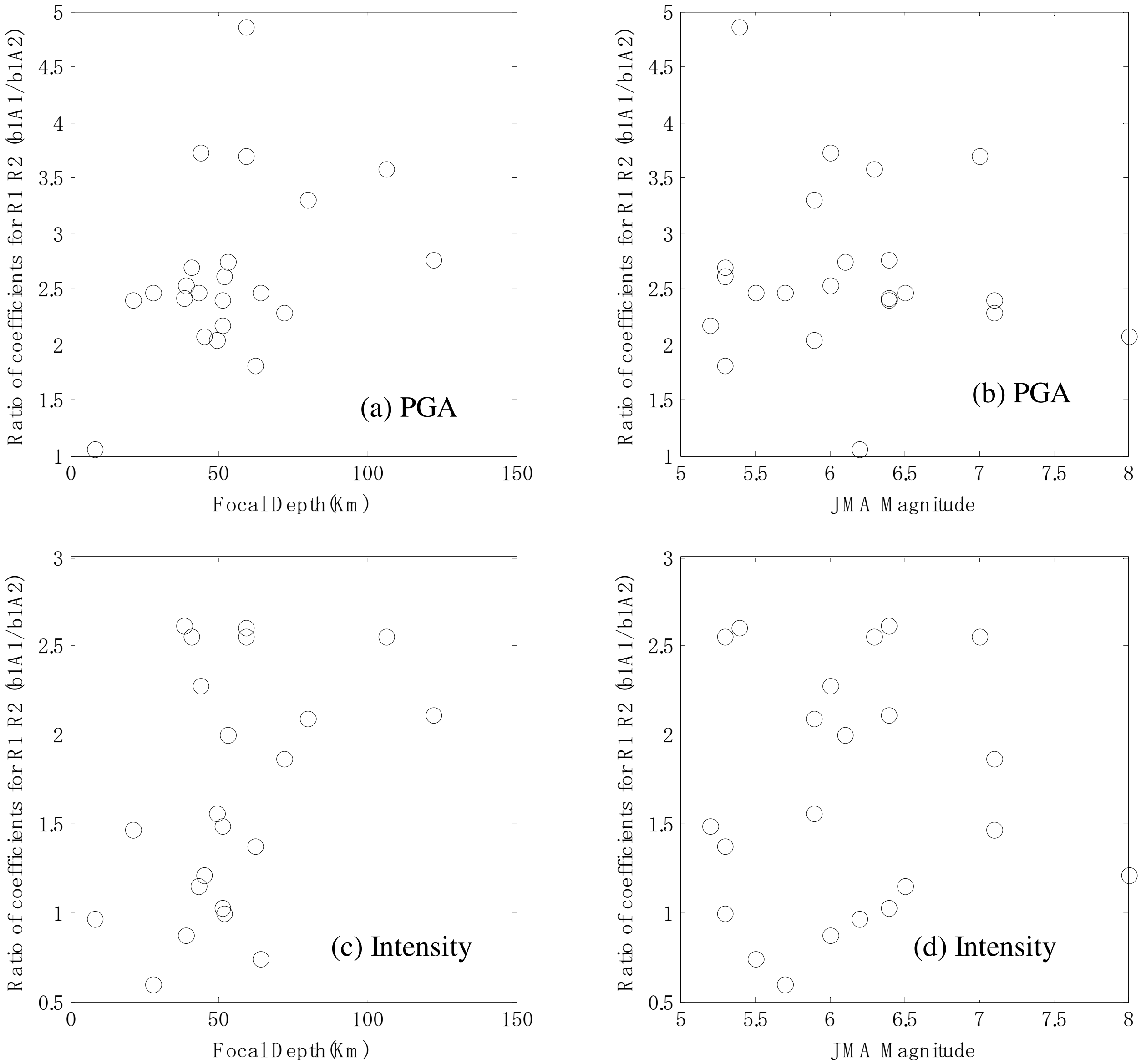

Figure 8. Relation between the ratio of coefficients b_{IA1}, b_{IA2} and (a)(c) focal depth, (b)(d) JMA Magnitude for earthquakes in which the data in the Japan-sea side is over whole 40%, and the data whose hypocentral distance is within 500km.

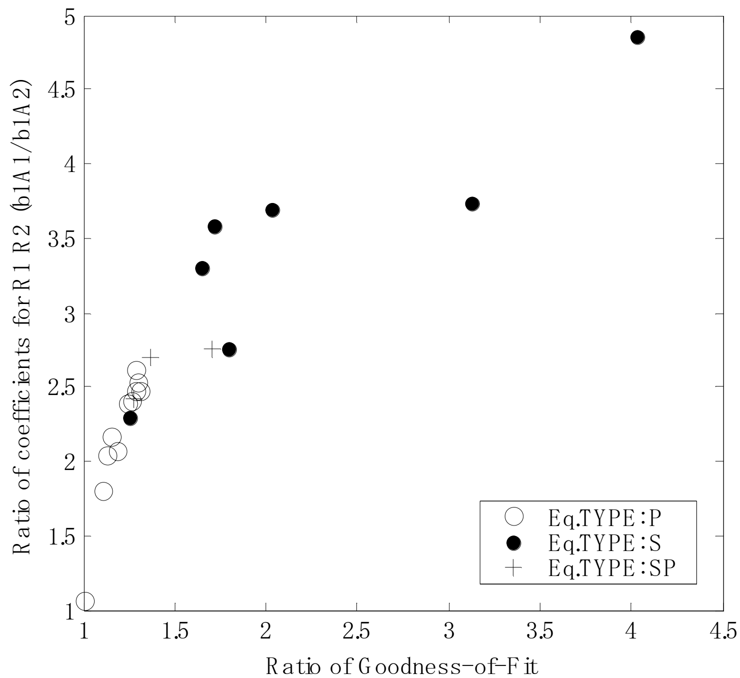

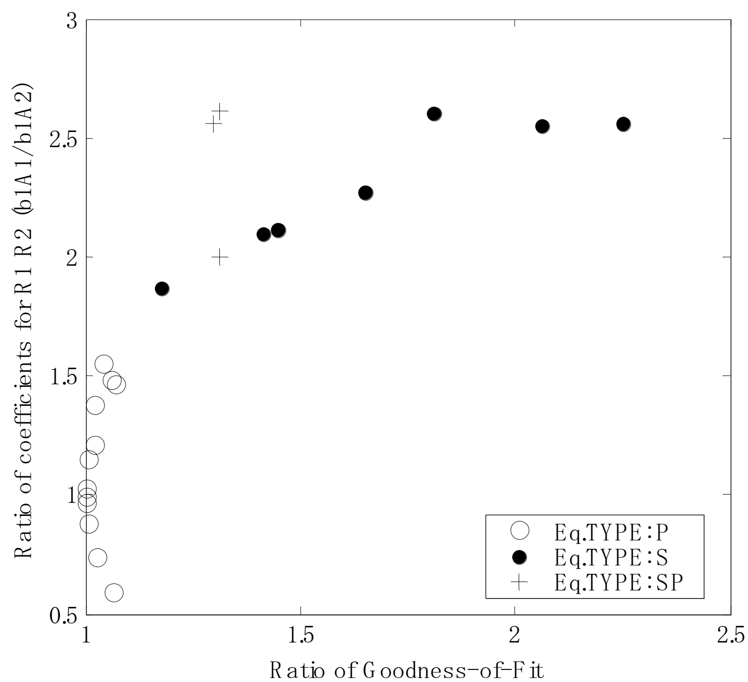

Figure 9. Relation between the ratio of goodness-of-fit (R^2 value of regression analysis) and ratio of coefficients b_{1A1}, b_{1A2}. (a) PGA, (b) Intensity.

The construction of the prediction expression

The above- mentioned possibility in which prediction accuracy is greatly improved by this technique became clear for the intra-plate earthquake, thereby the prediction expression in the intra-plate earthquake is constructed.

The attenuation model for PGA and instrumental intensity in this study are given by

$$\mathrm{Log}_{10}PGA=a_A*M_{JMA}+C_{2A1}-\log_{10}R-b_{2A1}R_1-b_{2A2}R_2 \tag{5}$$

$$I=a_I*M_{JMA}+C_{2I1}-2*\log_{10}R-b_{2I1}R_1-b_{2I2}R_2 \tag{6}$$

where the terms $\log_{10}R$ represent geometric spreading and terms bR represent anelastic attenuation. The coefficient of $\log_{10}R$ is 1.0 in the equation (5) is because the body wave is assumed. And since past coefficients in conversion formulas of the seismic intensity from acceleration are almost due to be 2.0's[5], the coefficient of $\log_{10}R$ in the equation (6) is constrained in 2.0. The two stages regression analysis [1,2,5] is used to obtain the coefficients in equations (5) (6). The first step b is determined, the second step a and C are determined. Determined equations by regression analysis are (7) and (8).

$$\mathrm{Log}_{10}PGA=2.56+0.217*M_{JMA}-\log_{10}R-0.000704*R_1-0.00389*R_2 \tag{7}$$

$$I=4.59+0.511*M_{JMA}-2*\log_{10}R-0.000945*R_1-0.00568*R_2 \tag{8}$$

DISCUSSIONS

Prediction expressions of PGA and instrumental intensity were obtained by the regression analysis of the above. R2 coefficient is lager than R1 coefficient, and it can be well understood that attenuation of earthquake motion differs in both sides in volcanic front. The equation becomes not prediction curve for the 2 variables but curved surface, and for example M8 case is shown in Figure 10 for Intensity. However, the comparison with the observation record is difficult, when it is given in the prediction curved surface. Therefore, θ required ratio of $R1$ and $R2$ length, namely ratio of $\Delta 1$ and $\Delta 2$, is introduced (Figure. 11). By utilizing this θ, gradients of curves of attenuation are decided, and curves in two dimensions for hypocentral distance can be expressed. Curves of attenuation in above-mentioned M8 earthquake can be shown like Figure 12. Like this, the prediction expression with multiple gradients for one earthquake is able to be constructed. Since θ is completely different from the correction factor of the site, and since it obtains it only from the position in hypocenter, V. F. and observation point, attention is necessary for changing by the earthquake location. Next, predicted intensity by this study is compared with observed seismic intensity. The 2003 Off-MIYAGI Earthquake (Eq. No.46) was intra-plate earthquake, and much damage was generated in Tohoku Region. Seismic intensity distribution maps are shown in Figure 13. Though the isoseismal becomes a concentric circle, if point source is assumed in past prediction expression, it becomes a similar shape in this technique with observed value. However, the predictive intensity in high level is lower than observed intensity. As a cause, that the ground amplification is not considered is also included. Conversely, if the cause is only ground amplification, there should be the tendency even in the low seismic intensity level. Then, the extraction condition of the data for the regression analysis tried to change, because there are problem in regression analysis. It is the largest epicentral distance of the data for the recurrence to change, and it gradually decreases the radius from 500km. It is clarified that the predicted seismic intensity is correct in the high seismic intensity level but incorrect in low level when the radius is decreased.

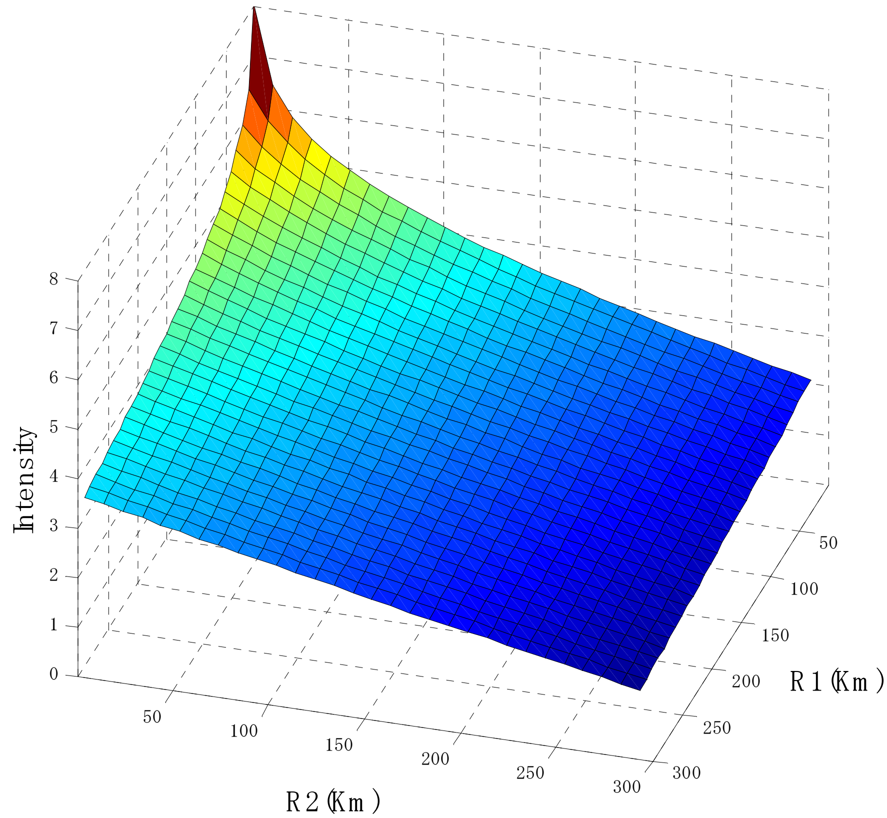

Figure 10. Attenuation curved surface in the case of M8.

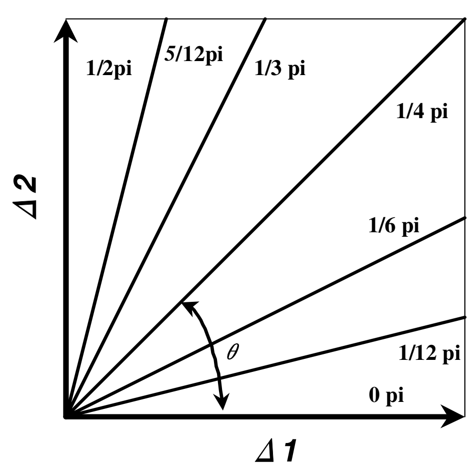

Figure 11. The scheme of the θ calculation from $\Delta 1$, $\Delta 2$.

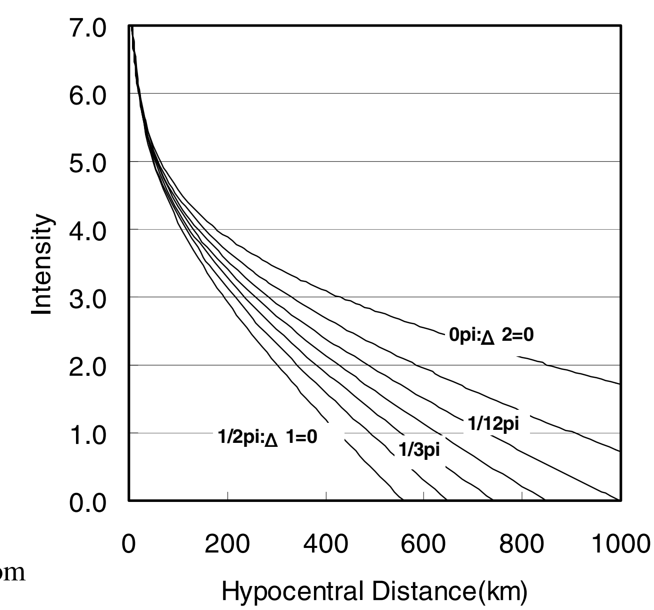

Figure 12. Attenuation relation in the every θ for the hypocentral distance in the case of M8.

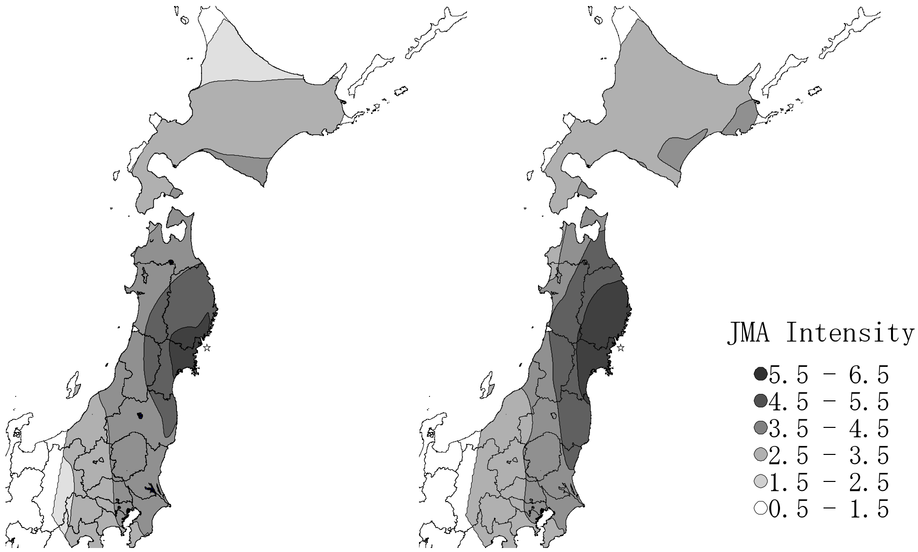

Figure 13. Isoseismal maps of 2003 Off-Miyagi Earthquake (Eq. No.46) , (a) predicted intensity by this study, (b) observed intensity by K-NET.

CONCLUSION

An attenuation formula that reflects the effect of a large-scale attenuation structure was obtained through deriving a regression formula dividing hypocentral distance by V.F.. It became clear that the longer the distance from the hypocenter to V.F., the smaller the attenuation for seismic intensity at an observation point. In the future, it aims at the development of the technique estimated from the high seismic intensity to low seismic intensity at the good accuracy by solving the problem of the largest epicentral distance of the data of regression. Moreover with some revision with ground condition, this formula would become a further accurate prediction method.

ACKNOWLEDGMENT

Kyoshin Net (K-NET) that provided the strong motion records used in this study is greatly acknowledged.

REFERENCES

1. Boore D.M, and Joyner W.B, “The empirical prediction of ground motion.” *Bull. Seism. Soc. Am* 1982; 72:S43-S60.
2. Fukushima Y, and Tanaka T. “A new attenuation relation for peak horizontal acceleration of strong earthquake ground motion in Japan”, *Bull. Seism. Soc. Am* 1991; 80: 757-783.
3. K-NET http://www.k-net.bosai.go.jp/k-net/index_en.shtml
4. Japan Meteorological Agency “Note on the JMA seismic intensity.” *Gyosei*, 1996:(in Japanese).
5. Shabestari, K.T, Yamazaki F. ”Attenuation Relationship of JMA Seismic Intensity Using Recent JMA Records.” *Proc. of the 10th Japan Earthquake Engineering Symposium* 1998; 10: 529-534.